ATMOSPHERIC EFFECTS ON RADARSAT-2 INTERFEROGRAMS OF TOLBACHIK VOLCANIC COMPLEX

Alexander Zakharov[1], Liudmila Zakharova[1], Polina Mikhaylyukova[2], Pavel Denisov[3]

[1] Kotelnikov Institute of Radioengineering and Electronics RAS, Russia, [2]Lomonosov Moscow State University, Russia, [3]JSC "Russian Space Systems", Russia

ABSTRACT

The results of the interferometric data processing of Canadian Radarsat-2 spaceborne synthetic aperture radar (SAR) acquired over Tolbachik volcanic complex in summer-fall 2013 are discussed. The phase difference deviations being revealed on the interferograms may be removed in some cases using the phase screen information generated using the weather stations archival meteorological records. The corruptions caused by cloud layers' heterogeneities, variations of air refraction coefficient height profiles, and fast variations of atmosphere conditions during dusk/down are the most complicating factors because of the lack of detailed description of clouds spatial structure and atmosphere parameters. One of most unexpected effects is atmosphere heterogeneity because of mixture of illuminated and shaded areas in mountainous regions in the case of interferometric SAR observations during dusk.

Index Terms— SAR, interferometry, RADARSAT-2, atmosphere, volcanic complex

1. INTRODUCTION

Atmosphere state is an important factor affecting the quality of the SAR information collected in space observations of Earth covers. Its properties are dependent on the daytime, season of the year, solar activity, latitude and longitude of observation area. In relatively short wavelength band like as C-band lower atmosphere layer, the troposphere, is dominating region. Interferometric observations are most sensitive to atmosphere conditions and signals temporal decorrelation in the case of repeated orbits interferometry scheme of observations.

Interferometric phase difference of signals acquired in SAR observations 1 and 2

$$\Delta\varphi_{12} = \varphi_1 - \varphi_2$$

is a sum of the next terms:

$$\Delta\varphi_{12} = \Delta\varphi_t + \Delta\varphi_d + \Delta\varphi_a + \Delta\varphi_n + \Delta\varphi_0,$$

where $\Delta\varphi_t$ - topographic phase, describing topographic height variations, $\Delta\varphi_d$ -small-scale spatial displacements of scattering surface (surface dynamics) between SAR observations, signal path length fluctuations in atmosphere $\Delta\varphi_a$, SAR receiver noise $\Delta\varphi_n$ and signal unknown initial phase $\Delta\varphi_0$.

Topographic phase $\Delta\varphi_t$ may be removed in a case of the topography data are available. The delineation of the component $\Delta\varphi_d$, describing scattering surface dynamics, is a task of differential SAR interefrometry. It is zero for the stable surfaces, consequently, remaining phase variations may be treated then as a manifestation of corrupting atmospheric effects. Vast amount of publications was devoted to the techniques allowing the estimation of the atmosphere impact onto interefrometric phase difference and its compensation (see, for example, [1]).

2. DATA DESCRIPTION AND STUDY AREA

To demonstrate corrupting effects of atmosphere on SAR interefrograms we used a set of RADARSAT-2 SAR data acquired in June-October 2013 from both ascending (6 scenes) and descending (6 scenes) repeated orbits with 24 days time interval between repeated observations. SRTM DEM data were used to correct topographic phase on SAR interefrograms. Meteorological information – atmospheric pressure, temperature and relative humidity were measured by local meteo stations in Kliuchi settlement located 60 km to the North and Kozyrevsk settlement located 40 km to the NNW from Tolbachik and taken from meteo site [2]. List of scenes, baselines between adjacent observations and solar illumination conditions for ascending and descending orbit are presented in Tables 1 and 2. Local observation time from ascending orbit was 20:05, and 08:22, next day, from descending orbit.

Table 1. Dates and sun location (ascending orbit).

Observ.date	Baseline, m	Sun elevation	Sun azimuth
20130601	71	11.6^0	292.4^0
20130625	47	13.3^0	292.2^0
20130719	230	11.6^0	289.9^0
20130812	187	6.6^0	286.8^0
20130905	361	-1.0^0	283.6^0
20130929		-10.0^0	280.0^0

Table 2. Dates and sun location (descending orbit).

Observ. date	Baseline, m	Sun elevation	Sun azimuth
20130605	44	27^0	90^0
20130629	23	27.4^0	88.3^0
20130723	99	24.3^0	90.0^0
20130816	108	19.6^0	94.3^0
20130909	123	13.7^0	100.7^0
20131002		7.0^0	107.6^0

Tolbachik is a volcanic complex on the Kamchatka Peninsula in the Far East of Russia. It consists of two volcanoes, Plosky (flat) Tolbachik (3080 m high) and Ostry (sharp) Tolbachik (3680 m high). Ostry Tolbachik has flat walls with inclination up to 15^0, its top is covered with permanent ice-snow layer. Ostry Tolbachik is a dormant stratovolcano with a ruined summit. It has two nested calderas of the Hawaiian type on the summit, the largest of them is 3 km in diameter. Inside it there is a young caldera with diameter of 1.8 km and a depth of about 400 m, which was formed during the eruption in 1975-1976. Last volcanic eruption of trombolian type started here on November 27, 2012. In the vicinity of the Tolbachik complex,13 km to the East, there are also Zimina Oval mountain (3000 m high) and Bolshaya Udina volcano (2900 m high), both present on RADARSAT-2 SAR images.

Typical Radarsat-2 amplitude image of the area is presented in Fig. 1a. A group of volcanic structures is seen in upepr right part of the image. Dark spot just below the image center is area of lava flows with flat cover in Tolbachinsky Dale. Most of the surrounding area near the volcanoes and Dale are covered with vegetetion of various density. Location of sparse vegetetion is delineated on the coherence maps because of higher temporal decorrelation. Two typical coherence maps from our processing activity are presented in Figs. 1b and 1c. Interferometric phase difference quality is dependent on a number of environmental and instrument-related factors. Temporal decorrelation is typically dominating factor in repeated orbits interefrometry scheme. Higher quality of coherence map in a pair 20130815-20130908 is defined by dry weather conditions during SAR observations with moderate air humidity. Ubrupt decrease of coherence on the map in pair 20130629-20130723 (right image) may be explained by dewfall in the case of 100% air humidity during sunrise on 20130723 and respective water drops condensation on the vegetation leaves.

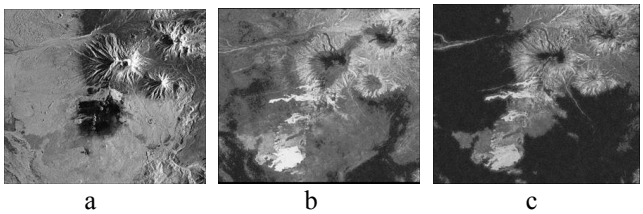

a b c

Fig. 1. Amplitude image (left) and two coherence maps (center and right).

The location of the areas with clear coherence decrease on the right map compared with central map is in good agreement with NDVI rise on the NDVI map (not presented here), which may serve as good indication of the vegetated areas location. Generally speaking, presense of dense vegetation covers in Tolbachik area is a serious corrupting factor all the year around, but summer time is preferable for interferometric observations [3].

Thorough study of the year 2013 eruption consequences as lava flows with differential SAR interferometry in 2013 was conducted in detail in [4]. 1-2 cm subsidence of the upper cover of hot lava belt (bright horizontal feature in the coherence map center) was detected. Presense of unwanted interferometric phase fluctuations because of atmosphere heterogeneity was one of most corrupting factors.

3. ATMOSPHERIC EFFECTS OBSERVED

3.1. Variations of height profiles of air refractivity

To demonstrate height variations of refractivity profile on the interferograms we will use the pair of Radarsat-2 images obtained on 15.08.2013 and 08.09.2016 [4]. The images were taken from ascending node at 20:20 o'clock local time. Elongation of signal path length ΔH in atmosphere is determined by spatial distribution and temporal variation of refractivity coefficient n:

$$\Delta H = \int_0^H (n-1)dh,$$

where H- geometrical path length. Refraction coefficient is very close to 1, so the reduced refraction coefficient N is widely used:

$$n = 1 + N.$$

In the Earth atmosphere N is dependent on pressure P, temperature T and water vapor partial pressure w as [5]:

$$N = \frac{77.6}{T}\left(P + \frac{4810w}{T}\right)10^{-6},$$

where pressure and water vapor partial pressure are counted in millibars, and temperature in degrees of Kelvin.

Elongation of signal path length for vertical propagation may be written as [5]:

$$\Delta H = 7.76 \cdot 10^{-5} \int_0^H \frac{P_a}{T} dh + 3.73 \cdot 10^{-1} \int_0^H \frac{w}{T^2} dh$$

or

$$\Delta H = \Delta H_{dry} + \Delta H_{wet},$$

where "dry" and "wet" mean dry atmosphere (water vapor free) and wet atmosphere (water vapor induced). The details of utilization the meteorological parameters in may be found elsewhere [6].

To correct for the phase shift caused by the difference in refractivity profiles in two SAR observations let's calculate

difference in elongations of path lengths dependent on signal penetration depth in atmosphere from volcano top $H_{\max}$ till the height h_c :

$$\Delta H_{12}(h_c) = \left(\int_{H_{\max}}^{h_c} N_1(h)dh - \int_{H_{\max}}^{h_c} N_2(h)dh \right) \frac{1}{\cos(\theta)},$$

where θ is incidence angle, and generate atmospheric phase screen for each interferogram pixel dependent on local height:

$$\Delta\varphi(h_c) = -\frac{4\pi}{\lambda}\Delta H_{12}(h_c),$$

where λ - signal wavelength.

In Fig 2 there are amplitude image and differential interferogram of Tolbachik area. Two interferometric strips around the volcano top are because of different atmosphere conditions during observations. Atmospheric phase screen constructed according to ground meteorological station data and results of interferogram correction are shown in Fig. 3. Some atmospheric remnants because of local deviations of atmosphere properties could not be described by point-wise ground station data, they remain visible on interferogram.

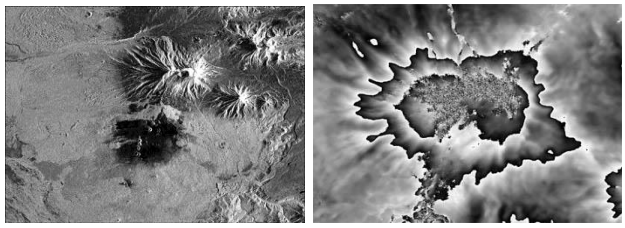

Fig. 2. Amplitude image (left) and differential interferogram before phase screen correction (right).

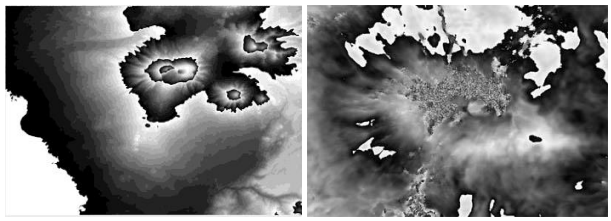

Fig. 3. Phase screen (left) and atmosphere corrected interferogram (right).

It should be underlined yet, that local meteorological station cannot be reliable source of the data to be used in atmospheric screen correction because of extremely sparse measurements. At the same time, other souses of meteorological information like as ERA-Interim reanalysis [7] being considered in our study were found to be extremely approximate in calculating atmospheric phase screen because of complication of atmospheric processes modeling in the case of rugged terrain in Kamchatka peninsula in general.

3.2. Signal path elongation in clouds

Dielectric constant of water vapor differs from 1, for that reason there is extra phase shift of the signal propagating in the cloud layer. The larger the signal travelling distance, the larger the phase shift. In the Fig. 4 there is no impact of cloud on the phase as the scattering point A lies above the cloud. Extra phase shift increases when scattering point moves from point A to B (beneath the cloud) because of elongation of signal path in cloud layer.

That's why on the phase profile along the western flank of volcano converted to signal path elongation (see Fig. 5) there is 2 cm increase from altitude 3200 m (cloud top in the first observation) till 1300 м (cloud bottom). As there is cloud layer in the second observation, its impact is subtracted in interferometric calculations. As a cloud bottom in a second observation was located at the altitude 800-1000 m, and we can see the decrease of the total signal path elongation from 2 to 1 cm.

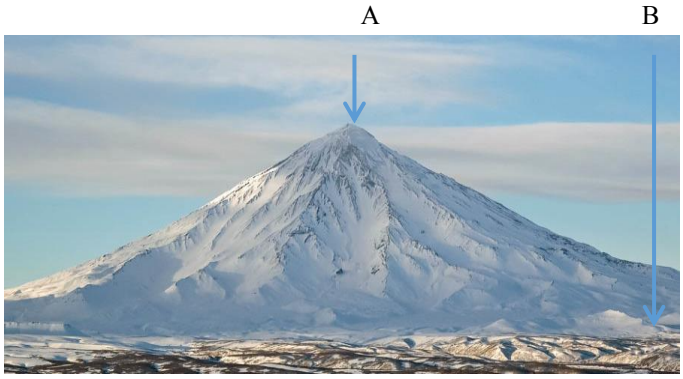

Fig. 4. An impact of the cloud on the signal path length

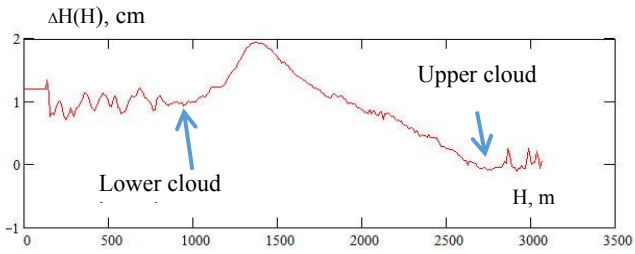

Fig. 5. Elongation of signal path length in the cloud.

3.3. Clouds inhomogeneities

Clouds inhomogeneities are the source of most frequent errors in differential SAR interferometry, as they introduce unwanted and unpredictable phase variations. Our estimations show that the phase variations across the clouds may exceed 100^0 (signal path variation for C-band SAR up to 1.2 cm), as it is seen in Fig. 6 displaying flat surface North-West from Tolbachik volcano, and cause serious

errors in DEM generation and estimations of surface dynamics. In given case ~1 cm one-way signal path variations are comparable with 1-2 cm subsidence of fresh lava surface being measured in [4].

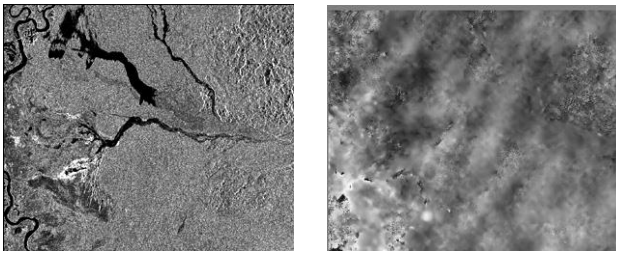

Fig.6. Amplitude image (left) and interferogram (right) with clouds impact.

3.4. Atmosphere heterogeneities during dusk

An influence of unequal heating of the rugged terrain surface by the sun during dusk and respectively air layer above on the signal phase was observed on interferograms obtained mainly in August-September, when Sun elevation angle during dusk was less than 14^0 (see Sun local coordinates in Table 1). In Fig. 7 there are amplitude image and interferogram obtained in the conditions mentioned.
Sun is illuminating the volcano complex here from upper left corner of the image. One can see a belt of decreased phase values behind the high volcanic complex (marked with arrow). The feature is not seen on June-July interferograms. It is unseen also on the data obtained from descending passes, when Sun was located to the right from the area on SAR image and its elevation angle is typically more than 10^0.

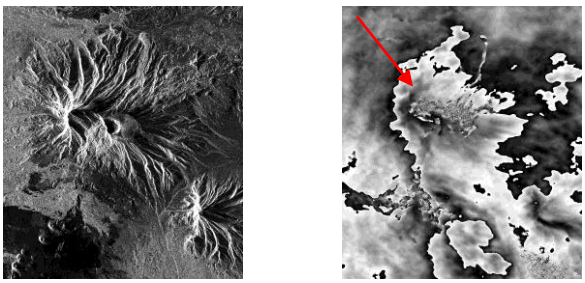

Fig.7. An influence of dusk observation conditions.

5. CONCLUSION

Obviously, the atmosphere is a source of large variety of errors in radar interferometric studies of Earth covers. There are tropospheric heterogeneities, instability of air refractivity height profiles because of varying weather conditions during observations. Also inequality of solar illumination of rugged terrain in the case of observations during down/dusk may be a serious confusing factor. Some of the errors may be minimized via averaging the stacks of interferograms obtained in different weather conditions, some of them (like as measurement errors over rugged terrain during dusk) may be avoided via thorough data selection.

ACKNOWLEDGMENTS

Authors are grateful to JAXA for PALSAR and PALSAR-2 data provided under RA3 and RA4 projects.
Authors acknowledge financial support of Russian Foundation for Basic Research (projects N 15-29-06003 and N 18-07-00816).

REFERENCES

[1] H. Berrada Baby, P. Golé, J. Lavergnat, A model for the tropospheric excess path length of radio waves // *Radio Science*, vol. 23, no. 6, pp. 1023–1038, November-December 1988.

[2] http://rp5.ru/

[3] Lundgren P., Kiryukhin A., Milillo P., Samsonov S, Dike model for the 2012–2013 Tolbachik eruption constrained by satellite radar interferometry observations //*Journal of Volcanology and Geothermal Research.* 2015. Vol. 307. pp. 79–88.

[4] Mikhaylyukova P.G., Tutubalina O.V., Mapping the volcanic eruptions using radar interferometry // *Modern problems of Earth remote sensing from Space*, vol. 13, no. 2, pp. 153-163, 2016, in Russian.

[5] Goldhirsh, J., et al, A Tutorial Assessment of Atmospheric Height Uncertainties for High-Precision Satellite Altimeter Missions to Monitor Ocean Currents // *IEEE Trans. on Geosci. and Rem. Sens.*, vol. ge-20, no. 4, October 1982.

[6] J. Askne, H. Nordius, Estimation of tropospheric delay for microwaves from surface weather data//*Radio Science*, vol. 22, no. 3, 379–386, May-June 1987.

[7] Dee, D. P., et al. (2011), The ERA-Interim reanalysis: Configuration and performance of the data assimilation system// *Q. J. R. Meteorol. Soc.*, *137*(656), pp. 553–597, doi:10.1002/qj.828.

[8] http://apps.ecmwf.int/datasets/data/interim-full-daily/levtype=sfc/